

HIERARCHICAL NANOSTRUCTURED NICKEL SULFIDE ARCHITECTURES THROUGH SIMPLE HYDROTHERMAL METHOD IN THE PRESENCE OF THIOGLYCOLIC ACID

MASOUD SALAVATI-NIASARI^{a, b*}, FATEMEH DAVAR^a, HAMID EMADI^a

^a *Institute of Nano Science and Nano Technology, University of Kashan, Kashan, P.O. Box 87317-51167, Islamic Republic of Iran*

^b *Department of Inorganic Chemistry, Faculty of Chemistry, University of Kashan, Kashan, P.O. Box 87317-51167, Islamic Republic of Iran*

Hierarchical nanostructures of β -NiS were successfully prepared by hydrothermal treatment of $\text{Ni}(\text{NO}_3)_2 \cdot 6\text{H}_2\text{O}$ and thioglycolic acid (TGA) at 180 °C. The as prepared β -NiS hierarchical nanostructures were characterized by X-ray diffraction (XRD), scanning electron microscopy (SEM), ultraviolet-visible (UV-vis) absorption spectroscopy, photoluminescence (PL) spectroscopy and Fourier transform infrared (FT-IR) spectra. The hierarchical nanostructures, with an average diameter of ~600 nm, were composed of short nanorods with a diameter of ~30 nm and a length of about 150 nm. On the basis of the experimental results and corresponding literatures, a possible growth mechanism of the NiS hierarchical nanocrystals is discussed. The obtained products have relatively high surface area, which favors the application in catalysis.

(Received December 1, 2010; accepted December 7, 2010)

Keywords: β -NiS, Hydrothermal; Hierarchical nanostructures; Electron microscopy.

1. Introduction

Transition metal sulfide materials nanostructures have been the focus of considerable interest due to their unique optical and electrical properties and their wide variety of potential applications in nanoscale devices such as electroluminescence, nonlinear optical devices, semiconductor, solid state secondary lithium battery cathodes, industrial catalysts, solar energy conversion, fluorescence devices and even light emitting diodes for flat-panel displays superconductor [1–6]. To the best of our knowledge, most advanced functions of inorganic materials strongly depend on their crystal geometrical phase, morphologies, and size. Up to now, many kinds of novel nanostructures such as nanotubes, nanoneedles, sea-urchin-like nanocrystallines, hollow microspheres, nanorods, nanowires, nanoprisms, nanoparticles, nanobelts, nanocubes and snowflakes like [7–16] metal sulfides nanocrystallines have been synthesized through chemical reactions of precursors at room or slightly elevated temperatures. However, with the growing interest in building advanced materials using nanosize building blocks, it remains a challenge to control the parameters of final products to fine-tune their properties.

Traditional method used to prepare transition metal sulfides is the direct reactions of the metal powders and sulfur in evacuated silica tubes at very high temperature. In the past decades, various approaches such as gas-phase reaction and thermal decomposition have been developed to fabricate metal sulfides nanomaterials [17, 18]. Among these approaches, many are based on high-temperature processes that generally required intricate processing and the use of high temperature for long periods of time, which may make the control of composition and morphology difficult. These difficulties have aroused extensive attention to the low-temperature synthesis of metal sulfides. In recent years, many low-temperature growth methods have been developed including molecular precursor, templated-mediated process, and solvothermal reaction [19–23].

*Corresponding author: salavati@kashanu.ac.ir

Recently, the hydrothermal method has been also reported to prepare metal sulfides nanostructural materials, which have potential advantages of relatively low cost, high purity, and controlled morphology [24–30]. In this paper, we demonstrated that the novel hierarchical nanostructured of β -NiS could be successfully synthesized in large quantities via a facile hydrothermal synthetic route using thioglycolic acid (TGA) and $\text{Ni}(\text{NO}_3)_2 \cdot 6\text{H}_2\text{O}$. Nowadays, there is obviously an increased emphasis on the green chemistry and chemical processes, which aim at the total elimination or at least the minimization of generated waste. Utilization of nontoxic environmentally benign solvents is of the key issues that merit important consideration in a green synthetic strategy. Herein, in this study, we present a convenient and green hydrothermal route to synthesize nickel sulfide nanostructures from $\text{Ni}(\text{NO}_3)_2 \cdot 6\text{H}_2\text{O}$ and thioglycolic acid (TGA), in which water was used as the environmentally benign solvent throughout the preparation.

2. Experimental

2.1. Materials and physical measurements

All reagents were analytic grade and used without further purification. The nitrogen adsorption and desorption isotherms at 77 K were performed on a Novia 3000 system after the sample was degassed at 30 °C overnight. XRD patterns were recorded by a Rigaku D-max C III, X-ray diffractometer using Ni-filtered $\text{Cu K}\alpha$ radiation. Scanning electron microscopy (SEM) images were obtained on Philips XL-30ESEM equipped with an energy dispersive X-ray spectroscopy. (FE-SEM) images were obtained on HITACHI S-4160. Fourier transform infrared (FT-IR) spectra were recorded on Shimadzu Varian 4300 spectrophotometer in KBr pellets. The electronic spectrum of the sample was taken on a Shimadzu UV–visible scanning spectrometer (Model 2101 PC). Room temperature photoluminescence (PL) was studied on an F-4500 fluorescence spectrophotometer. The elemental analysis (carbon, hydrogen and nitrogen) of the materials was obtained from Carlo ERBA Model EA 1108 analyzer. Raman spectrum was recorded on a Bruker FT–Raman spectrometer model RFS 100/S equipped with an Nd:YAG laser (maximal power: 5 W; laser wavelength: 1.64 μm). The specific surface areas of as-prepared NiS were determined from the nitrogen absorption data at liquid nitrogen temperature using the BET technique by means of a Micromeritics ASAP 2000 apparatus.

2.2. Preparation of hierarchical nanostructured of β -NiS

In a typical procedure, different molar ratios of $\text{Ni}(\text{NO}_3)_2 \cdot 6\text{H}_2\text{O}$ and thioglycolic acid (TGA) were mixed in 200 mL distilled water under stirring. After 30 min the final mixed solution was sealed into a 250 mL Teflon-lined stainless steel autoclave, and heated at 180 °C for 6–24 h in an electric oven (Table 1). The autoclave was cooled to the room temperature naturally when it is up to the required reaction time. The product was washed with distilled water and absolute ethanol three times to remove the excessive reactants and byproducts, followed by drying in an oven at 60 °C for 8 h.

Table 1. Reaction conditions for synthesis of NiS.

Sample no.	Molar ratio(Ni^{2+} :TGA)	Time (h)	Temperature (°C)	Thermal stability
1	1:1	12	180	-----
2	1:2	12	180	-----
3	1:3	12	180	-----
4	1:3	24	180	-----
5	1:3	6	180	-----
6	1:3	24	180	160 °C for 12h

3. Results and discussion

The typical XRD pattern of the product prepared at 180 °C is shown in Fig. 1a. All peaks can be clearly indexed to β -NiS. No obvious diffraction peaks from other impurities, such as Ni₂S₃, Ni₃S₄, and Ni₉S₈, were observed in the XRD pattern. The space group of the as-prepared products is $R\bar{3}m$, and the cell parameters ($a=9.63$ Å and $c=3.16$ Å) are in good agreement with the literature data (JCPDS No. 12-0041).

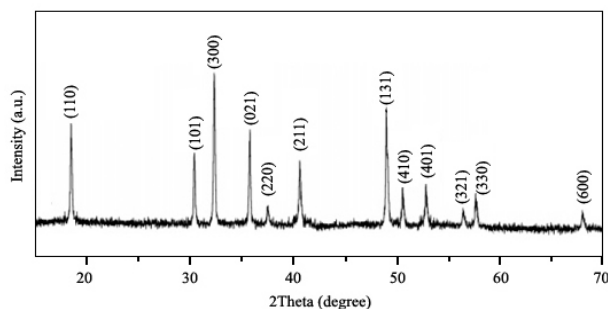


Fig. 1. XRD pattern of the product prepared at 180 °C for 24 h (sample no. 4).

The morphology of the samples was further examined by field emission scanning electron microscopic (FE-SEM) and scanning electron microscopic (SEM). SEM and FE-SEM images of as-synthesized NiS are shown in Figs. 2 and 3. FE-SEM images of samples with different molar ratio and constant reaction time and temperature are presented in Fig. 2. Careful observation shows that the surfaces of these crystals are covered by hierarchical structures. The best result was achieved at the condition mentioned for sample no. 2. These images imply that the best ratio molar is 1:2 (Ni²⁺:TGA) and by increasing the ratio molar the crystal will be larger and below this ratio hierarchical structures have not been constructed well. The hierarchical nanostructures (sample no. 2), with an average diameter of ~600 nm, were composed of short nanorods with a diameter of ~30 nm and a length of about 150 nm. Fig. 3 shows SEM images of as-synthesized samples with different reaction time and constant molar ratio and temperature. Comparison between these images suggested that the desired product is obtain at reaction time 12 h and by increasing reaction time to 24 h the samples cleave to each other. It is clear that at this molar ratio we cannot obtain hierarchical structures and changes in reaction time do not have significant effect on synthesis hierarchical structures at this molar ratio.

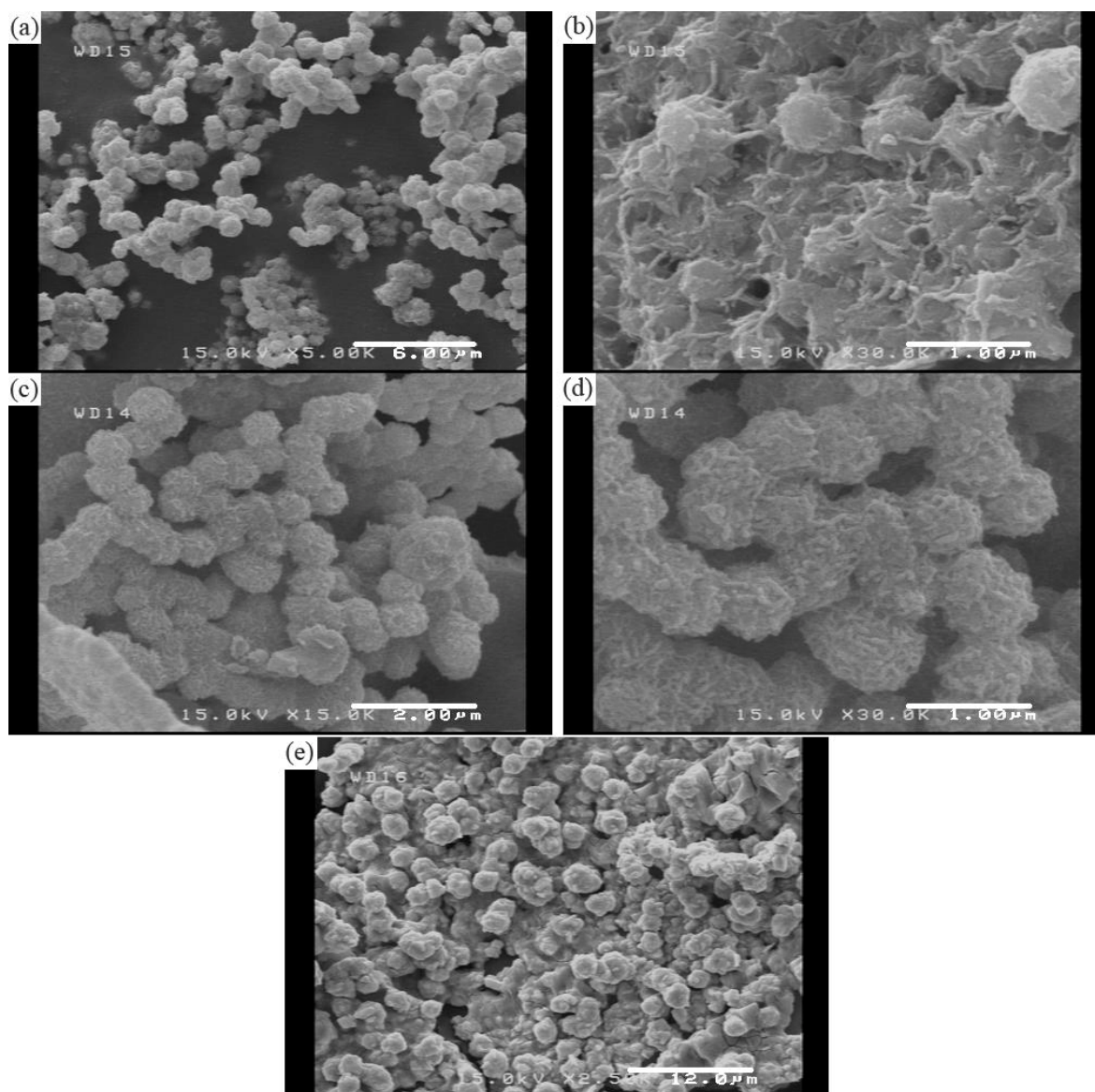


Fig. 2. FE-SEM images at constant reaction time (12 h) and temperature (180 °C) with different molar ratio: (a, b) 1:1 (sample no. 1), (c, d) 1:2 (sample no. 2) and (e) 1:3 (sample no. 3).

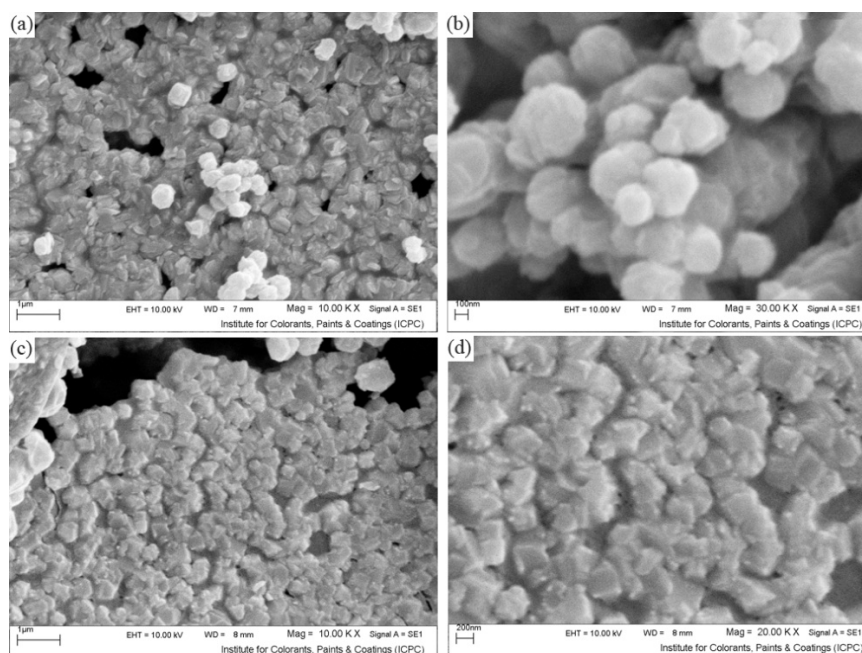


Fig. 3. SEM images at constant molar ratio (1:3) and temperature (180 °C) with different reaction time: (a, b) 24 h (sample no.4) and (c, d) 6 h (sample no.5).

Fourier transformed infrared (FT-IR) of the as-synthesized samples were performed in order to investigate that the surface of particle is capped with organic material or not. The IR spectrum of the samples obtained from the as synthesized NiS Fig. 4a shows impurity that can arise from TGA that has been absorbed on the surface of the sample. The peak at 3429 cm^{-1} could be ascribed to the absorption of H_2O in the sample. From the FT-IR spectrum, carboxylate are confirmed to be present in the as-synthesized products. The strong absorption peaks at 1626 cm^{-1} should be corresponded to the $-\text{COOH}$ asymmetry stretching vibration. From the result of FT-IR analysis, it is suggested that the organic component $-\text{CH}_2\text{COOH}$ should exist in the composite. We believe that these absorption peaks are close to those of $(\text{CdS})_m(\text{SHCH}_2\text{COOH})_k^{2+}$. Associating all of these results, the whole process can be expressed as followed (Scheme 1). At the first step TGA was introduced to Ni^{2+} and produce (2), this product generate (3) via the following route:



At the final step $(\text{NiS})_m(\text{NiSHCH}_2\text{COOH})_k^+$ changed to the NiS by hydrothermal. As we mentioned above, FT-IR spectrum of as prepared product showed impurity. To remove impurities we dispersed sample in 100 mL of water and then put the mixture in a 150 mL Teflon-lined stainless steel autoclave, and heated at 160 °C for 12 h in an electric oven (thermal stability) (sample no. 6). The product was washed with distilled water and absolute ethanol several times to remove the excessive impurities. FTIR of the sample after thermal stability is shown in Fig. 4b. From FTIR spectrum of the sample after thermal stability it is clear that there is some impurity yet that arise from TGA capped at the surface of the product. Two SEM images that are presented in Schem.1 show morphology of samples after this step. These images show that after this step the particles have hierarchical structures morphology and thermal stability reaction did not change their morphology but made their size distribution smaller.

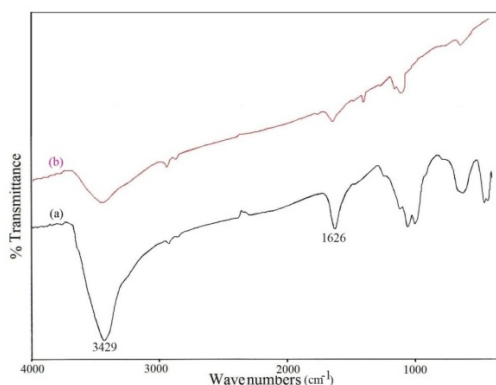
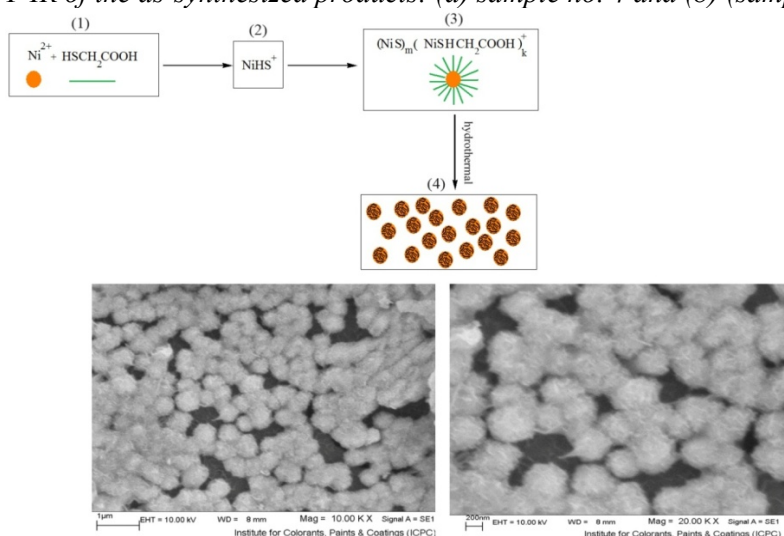


Fig. 4. FT-IR of the as-synthesized products: (a) sample no. 4 and (b) (sample no. 6).



Schem.1. Proposed mechanism for synthesis of NiS.

The Raman spectrum of hierarchical nanostructured β -NiS shown in Fig. 5 was obtained at room temperature. It is noticed that there are five obvious vibrational modes at 143, 240, 299, 345, and 371 cm^{-1} for sample no. 2 (Fig. 5), which is in agreement with the literature data [31, 32]. However, some vibrational modes could not be observed. This may be due to the small size effect of the nanomaterials since Raman vibrational modes mightily depend on the vibration of the crystal lattice [33, 34]. When the size of the crystal is reduced to the nanoregion, the atom arrangement inside the crystal lattice may change compared with that of the bulk materials, which would affect the vibrational modes.

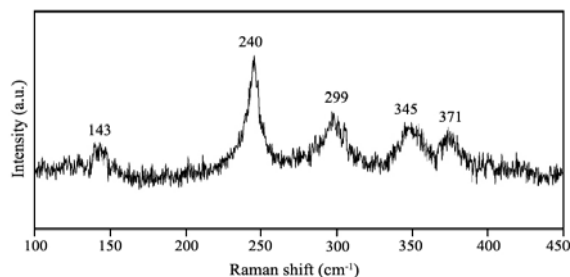


Fig. 5. Raman spectra of NiS nanostructures (sample no. 2)

It is well known that the absorption spectrum can characterize the dispersivity of semiconductor nanostructures. Fig. 6 shows the UV-vis absorption spectrum of the as-prepared hierarchical NiS nanostructures. A strong peak centered at round 200 nm was detected, and also it was very interesting that were observed two weak shoulders around 226 nm and 272 nm in UV-vis absorption spectrum of NiS hierarchical nanostructures. These data are in agreement with

results reported by Shen [35]. The absorption spectrum shows an obvious blue shift compared with that of bulk NiS (~ 2.1 eV).

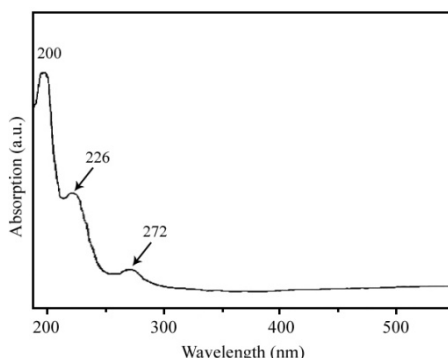


Fig. 6. UV-vis absorption spectrum of the NiS nanostructures (sample no. 2).

The optical property of the product was also investigated. Fig. 7 shows the fluorescence spectrum of the hierarchical β -NiS sample (sample no.2). Under PL excitation at 274 nm, there was a broad emission around 400 nm, and the top of the emission peak was separated into two peaks located, respectively, at 390 and 415 nm, which may be due to electronic transitions caused by defects in the interfacial region1 [4,15]. The PL spectrum of the NiS hierarchical nanostructures indicate a broad emission at 390–415 nm which is shorter than the submicrometer NiS hollow spheres for the smaller size [36], indicating NiS nanocrystals synthesized in this work is in the quantum confinement regime as well. The highly structured shape of the emission suggests that the emission of NiS nanocrystal comes from intermolecular exciton interactions rather than the interaction of excimers [37, 38].

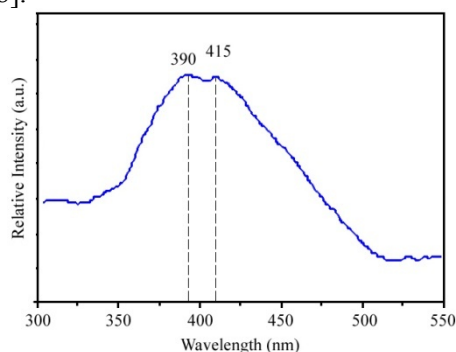


Fig. 7. Fluorescence spectrum ($\lambda_{ex} = 274$ nm) of hierarchical NiS (sample no. 2).

The specific surface area of the as-prepared NiS calculated by the BET method is ca. 83 m^2/g for hierarchical nanostructured of β -NiS. The result is much higher than the reported value [39] and indicates that the products are applicable for catalysis.

4. Conclusions

In summary, NiS hierarchical nanostructures were prepared directly by a hydrothermal route using $\text{Ni}(\text{NO}_3)_2 \cdot 6\text{H}_2\text{O}$ and thioglycolic acid (TGA) as starting materials in water at 180 $^\circ\text{C}$ for 24 h. FE-SEM and SEM characterizations revealed that the products were hierarchical nanostructures with an average diameter of ~ 600 nm, composed of short nanorods. The effect of the molar ratio and time of reaction on the morphology were investigated, and a possible formation mechanism for the hierarchical NiS was proposed. The optical properties of the NiS products were evaluated by UV-vis spectroscopy at ambient temperature. TGA molecules absorbed on the surface of nanocrystals played important roles in the process of assembling, which can generate a

regular interparticle spacing and offer nanocrystals with a strong tendency to assemble into 2D arrays with regular checked pattern on substrates. Since the method used is simple, cheap, air-stable, nontoxic, and readily available for many metal elements, this synthesis may represent a rather environmentally friendly and general approach towards many other metal sulfide nanocrystals. Furthermore, this research may promise both adequate academic and practical interest in the development of synthetic methodologies for inorganic nanocrystals, and in the expansion of their potential applications.

Acknowledgment

Authors are grateful to the Council of the University of Kashan for providing financial support to undertake this work.

References

- [1] V.I. Klimov, A.A. Mikhailovsky, S. Xu, A. Malko, J.A. Hollingsworth, C.A. Leatherdale, H.-J. Eisler, M.G. Bawendi, *Science* **290**, 314–316 (2000).
- [2] C.L. Czekaj, M.S. Rau, G.L. Geoffroy, T.A. Guiton, C.G. Pantano, *Inorg. Chem.* **27**, 3267–3269 (1988).
- [3] R. Tenne, L. Margulis, M. Genut, G. Hodes, *Nature* **306**, 444–446 (1992).
- [4] H. Li, L. Chai, X. Wang, X. Wu, G. Xi, Y. Liu, Y.T. Qian, *Cryst. Growth Design* **7**, 1918–1922 (2007).
- [5] J. Chen, S.L. Li, Q. Xu, K. Tanaka, *Chem. Commun.* 1722–1723 (2002).
- [6] H.S. Yang, P.H. Holloway, B.B. Ratna, *J. Appl. Phys.* **93**, 586–592 (2003).
- [7] C.N.R. Rao, M. Nath, *Angew. Chem.* **114**, 3601–3604 (2002).
- [8] Z.P. Qiao, G. Xie, J. Tao, Z.Y. Nie, Y.Z. Lin, X.M. Chen, *J. Solid State Chem.* **166**, 49–52 (2002).
- [9] C.J. Barrelet, Y. Wu, D.C. Bell, C.M. Lieber, *J. Am. Chem. Soc.* **125**, 11498–11499 (2003).
- [10] A. Ghezelbash, M.B. Sigman, B.A. Korgel, *Nano Lett.* **4**, 537–542 (2004).
- [11] Q.Y. Lu, F. Gao, S. Komarneni, *J. Am. Chem. Soc.* **126**, 54–55 (2004).
- [12] M. Salavati-Niasari, M.R. Loghman-Estarki, F. Davar, *Chem. Eng. J.* **145**, 346–350 (2008).
- [13] M. Salavati-Niasari, F. Davar, *Mater. Lett.* **63**, 441–443 (2009).
- [14] F. Mohandes, F. Davar, M. Salavati-Niasari, *J. Magn. Magn. Mater.* **322**, 872–877 (2010).
- [15] M. Salavati-Niasari, M. Bazarganipour, F. Davar, *J. Alloys Compd.* **489**, 530–534 (2010).
- [16] B. Geng, X. Liu, J. Ma, Q. Du, *Mater. Sci. Eng. B* **145**, 17–22 (2007).
- [17] M. Nath, C.N.R. Rao, *Adv. Mater.* **13**, 283–286 (2001).
- [18] P. Boudjouk, M.P. Remington Jr., D.G. Grier, B.R. Jarabek, G.J. Maccarthy, *Inorg. Chem.* **37**, 3538 (1998).
- [19] D.M. Wilhelmy, E. Matijeve, *J. Chem. Soc. Faraday Trans.* **80**, 563–570 (1984).
- [20] Y. Li, J.H. Wan, Z.N. Gu, *Mater. Sci. Eng. A* **286**, 106–109 (2000).
- [21] Y.D. Li, H.W. Liao, Y. Ding, Y.T. Qian, L. Yang, G.E. Zhou, *Chem. Mater.* **10**, 2301–2303 (1998).
- [22] X.F. Qian, X.M. Zhang, C. Wang, Y. Xie, Y.T. Qian, *Inorg. Chem.* **38**, 2621–2623 (1999).
- [23] J. Hu, B. Deng, K. Tang, Q. Lu, R. Jiang, Y.T. Qian, *Solid State Sci.* **3**, 275–278 (2001).
- [24] M. Salavati-Niasari, M.R. Loghman-Estarki, F. Davar, *J. Alloys Compd.* **475**, 782–788 (2009).
- [25] M. Salavati-Niasari, D. Ghanbari, F. Davar, *J. Alloys Compd.* **492**, 570–575 (2010).
- [26] M. Salavati-Niasari, F. Davar, M.R. Loghman-Estarki, *J. Alloys Compd.* **494**, 199–204 (2010).
- [27] M. Salavati-Niasari, A. Sobhani, F. Davar, *J. Alloys Compd.* **507**, 77–83 (2010).
- [28] M. Salavati-Niasari, D. Ghanbari, F. Davar, *J. Alloys Compd.* **488**, 442–447 (2009).
- [29] M. Salavati-Niasari, M. Bazarganipour, F. Davar, *J. Alloys Compd.* **499**, 121–125 (2010).
- [30] M. Salavati-Niasari, F. Davar, M.R. Loghman-Estarki, *J. Alloys Compd.* **481**, 776–780 (2009).

- [31] J. Dong, Z. Cheng, S.W. Zha, M.L. Liu, *J. Power Sources* **156**, 461–465 (2006).
- [32] D.W. Bishop, P.S. Thomas, A.S. Ray, *Mater. Res. Bull.* **33**, 1303–1306 (1998).
- [33] M. Yoshikawa, M. Murakami, K. Matsuda, T. Matsunobe, S. Sugie, K. Okada, H. Ishida, *J. Appl. Phys.* **98**, 063531–063533 (2005).
- [34] M. Holtz, W.M. Duncan, S. Zollner, R. Liu, *J. Appl. Phys.* **88**, 2523–2528 (2000).
- [35] X. Shen, J. Sun, G. Wang, J. Park, K. Chen, *Mater. Res. Bull.* **45**, 766–771 (2010).
- [36] Y. Hu, J.F. Chen, W.M. Chen, X.H. Lin, X.L. Li, *Adv. Mater.* **15**, 726–729 (2003).
- [37] X. Jiang, Y. Xie, J. Lu, L. Zhu, W. He, Y. Qian, *Adv. Mater.* **13**, 1278–1281 (2001).
- [38] Z. Wu, C. Pan, T. Li, G. Yang, Y. Xie, *Cryst. Growth Design*, **7**, 2454–2459 (2007).
- [39] A. Olivas, J. Cruz-Reyes, M. Avalos, V. Petranovskii, S. Fuentes, *Mater. Lett.* **38**, 141–144 (1999).